Synthesis and characterization of graphene oxide from tropical fruit peel waste using liquid phase exfoliation sonication and magnetite as catalyst

W. Widyawidura[a,*], Y. K. Pradani[a], M. N. Aridito[a], L. E. Ibrahim[b], H. P. Prihanto[b], and W. S. B. Dwandaru[b,c]

[a]*Department of Environmental Engineering, Universitas Proklamasi 45, Yogyakarta 55281, Indonesia,*
[b]*Department of Physics Education, Universitas Negeri Yogyakarta, Yogyakarta 55281, Indonesia,*
[c]*Nanomaterial for Advanced Waste Management and Sustainable Environment Optimization,*
Jl. Colombo No. 1, Karangmalang, Yogyakarta 55281, Indonesia,
[*]*email: wirawidura@up45.ac.id*

Received 16 December 2025; accepted 17 March 2026

Graphene oxide (GO) is a highly versatile nanomaterial with remarkable structural, electrical, and surface properties, making it useful for energy storage, catalysis, and biomedical applications. In this study, durian peel waste was used as a carbon-rich precursor for the synthesis of GO, offering a sustainable and cost-effective route to nanomaterials. The raw material was first subjected to pyrolysis at 400°C in a rocket stove reactor to produce biochar. The resulting carbon was processed using liquid-phase acid sonication (LAS) and ultrasonication to synthesize GO. The samples were characterized by X-ray diffraction (XRD), Raman spectroscopy, and scanning electron microscopy (SEM). The XRD patterns confirmed the presence of oxidized graphitic structures, Raman spectra revealed the characteristic D and G bands with an increased ID/IG ratio indicating the formation of structural defects, and SEM images showed wrinkled, layered morphologies typical of GO sheets. These results demonstrate that tropical fruit waste can be valorized into advanced nanomaterials through environmentally friendly processing, highlighting the dual benefits of waste reduction and material innovation.

Keywords: Graphene oxide; durian peel waste; pyrolysis; liquid-phase acid sonication; ultrasonication; XRD; Raman spectroscopy; SEM.

DOI: https://doi.org/10.31349/RevMexFis.72.051004

1. Introduction

The conventional synthesis of graphene oxide (GO) remains largely dominated by graphite-based chemical approaches, such as the Hummers method and its subsequent modifications, which involve the use of strong oxidizing agents including $KMnO_4$ and concentrated H_2SO_4 [1,2,3]. Despite their effectiveness, these methods pose significant environmental and occupational safety concerns. Moreover, they rely heavily on commercially sourced graphite, which is relatively expensive and non-renewable. An alternative strategy that addresses several of these limitations is the liquid phase exfoliation (LPE) method. LPE mitigates the need for hazardous chemical oxidants by mechanically exfoliating graphite layers through physical forces, thereby offering a comparatively greener and safer approach [4,5]. Nevertheless, the synthesis of GO via LPE still predominantly depends on commercial graphite as the primary carbon source.

In recent years, there has been a growing shift toward the utilization of biomass, such as basil seeds, wheat straw, rice husks, peanut shells, and other agricultural residues as sustainable and renewable carbon precursors for the production of graphene-based materials [6,7,8]. The LPE technique has demonstrated its capability to convert biomass-derived precursors, for instance rice stem, into graphene-like materials, providing a viable alternative to conventional graphite feedstocks [9]. These developments highlight the necessity for further optimization and advancement of the LPE method to enhance its efficiency, scalability, and applicability in sustainable graphene production.

On the other hand, durian (Durio zibethinus), often referred to as the "king of fruits," is one of the most popular tropical fruits in Southeast Asia, particularly in countries such as Indonesia, Malaysia, and Thailand. With the growing consumption and industrial-scale processing of durian, a substantial amount of durian peel waste is generated annually, accounting for approximately 60-70% of the total fruit mass [10]. This organic residue is typically discarded in open areas or landfills, leading to environmental problems such as unpleasant odor, methane emission from anaerobic decomposition, and vector attraction [11].

The accumulation of durian peel waste has therefore become a pressing environmental concern in durian-producing regions of Southeast Asia, prompting efforts to valorize this biomass into high-value carbon-based materials. To address this issue, durian peel waste can be valorized through thermochemical conversion, one of which involves transforming it into biochar via controlled thermal treatment at specific temperatures. Previous studies have reported that durian peel waste can be successfully converted into biochar at relatively low temperatures, typically in the range of 300°C to 600°C [12,11]. Biochar derived from organic waste through thermal treatment within this temperature range exhibits significant potential as a sustainable alternative to commercial graphite in the synthesis of graphene oxide (GO) [7]. Its utilization not only reduces reliance on mined graphite but also promotes a more environmentally benign and circular approach to GO production.

To further improve the efficiency of the LPE process, recent studies have investigated the integration of Fe_3O_4

nanoparticles as a complementary exfoliation agent, working synergistically with linear alkylbenzene sulfonate (LAS) to enhance layer delamination and dispersion stability. The shear forces generated by the collision of Fe_3O_4 particles with graphite surfaces synergistically enhance the ultrasonication process and the surface tension reduction effect induced by LAS, promoting more effective exfoliation of graphite layers and leading to improved graphene yield [13,4]. The shear forces induced by Fe_3O_4 are not limited to the exfoliation of graphite layers but have also demonstrated the capability to delaminate other layered materials, such as boron nitride surfaces [14]. This versatility highlights the potential of Fe_3O_4 as an effective exfoliation agent in LPE, particularly in the context of GO synthesis.

Based on the identified research gaps and proposed solutions drawn from previous studies, this work aims to convert graphite derived from durian peel waste via low-temperature pyrolysis into graphene oxide (GO) using a modified liquid-phase exfoliation (LPE) method. The modification involves a synergistic combination of linear alkylbenzene sulfonate (LAS) and Fe_3O_4 to facilitate mechanical delamination of graphite layers under ultrasonic bath irradiation. The crystallinity, defect structure, and morphological characteristics of the synthesized GO will be systematically characterized using X-ray diffraction (XRD), Raman spectroscopy, and scanning electron microscopy (SEM).

2. Materials and methods

Durian peels were collected, cleaned, and dried before pyrolysis. The pyrolysis process using a rocket stove reactor was conducted for a total duration of approximately four hours. During the first 30 minutes, the temperature gradually increased from ambient temperature (around 30°C) to approximately 200°C. In the next 15 minutes (at around the 45^{th} minute), the temperature rose further to about 300°C. After one hour of operation, the temperature reached the target 400°C and was maintained at this level. At around 1.5 hours into the process, the release of pyrolysis gas was observed, indicating the active decomposition of the durian peel biomass. The produced pyrolysis gas was self-combusted and used as a supplementary heat source, allowing the external burner to be turned off. The combustible gas continued to evolve for approximately one hour before gradually ceasing, during which the reactor temperature slowly decreased to around 300°C after about 2.5 to 3 hours of processing. Once the pyrolysis gas was depleted, the external burner was reignited and maintained for an additional hour to ensure the completion of the carbonization process, resulting in a total reaction time of around four hours. Similar pyrolysis-based strategies have been reported to yield biochar rich in aromatic domains that can serve as a precursor for further oxidation [15].

A total of 250 mL of distilled water was mixed with 1 mL of linear alkylbenzene sulfonate (LAS) by stirring for 5 minutes at room temperature. Then, 1 gram of durian peel-derived graphite powder was slowly added to the solution and stirred for 30 minutes at room temperature. The resulting mixture was sonicated for 2 hours at 10-minute intervals with 2-minute pauses between each cycle. After sonication, the solution was filtered to separate the precipitate from the liquid. Finally, the filtrate was microwaved until completely dried to obtain graphene oxide (GO) powder. This carbonized material was then subjected to liquid-phase acid treatment, where the introduction of oxygen-containing groups increased the interlayer spacing of the carbon matrix [16]. Subsequently, ultrasonication promoted mechanical exfoliation, separating stacked graphitic layers into nanosheets of GO [17].

Characterization was performed to confirm structural transformation. XRD analysis was employed to identify the emergence of oxidation-related peaks and increased d-spacing, which are typical signatures of GO [18] [10]. Raman spectroscopy was used to detect the D band associated with defects and the G band related to graphitic domains, with the ID/IG ratio serving as an indicator of disorder and successful oxidation [19]. SEM provided direct evidence of morphological transformation, allowing observation of surface wrinkling and layered sheet structures that are characteristic of GO [20].

3. Results and discussion

GO was synthesized from durian peel waste graphite using the LPE method through the synergistic effects of LAS surfactant, Fe_3O_4, and cavitation. The pyrolysis of organic waste (in this study, durian peel waste pyrolyzed at 400°C) generally produces carbon with an amorphous or turbostratic nature (disordered graphitic structure), as low to intermediate temperature pyrolysis is insufficient to rearrange carbon atoms into a well-ordered crystalline graphite structure, resulting in amorphous carbon being the dominant structure in the initial pyrolysis product [21]. Thus, the incorporation

FIGURE 1. GO sample synthesized with Fe_3O_4 assistance.

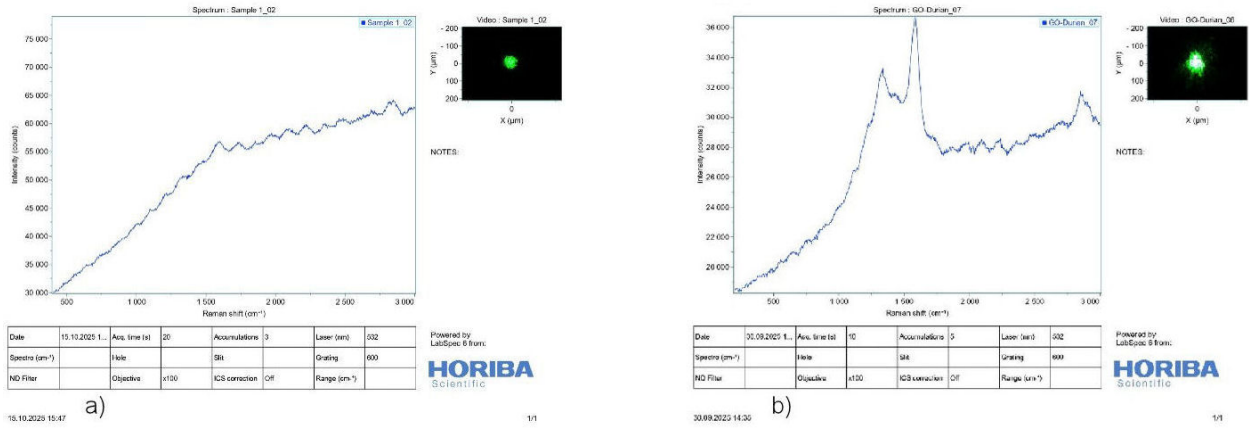

FIGURE 2. Raman spectra of GO: a) GO without Fe_3O_4 assistance and b) GO with Fe_3O_4 assistance.

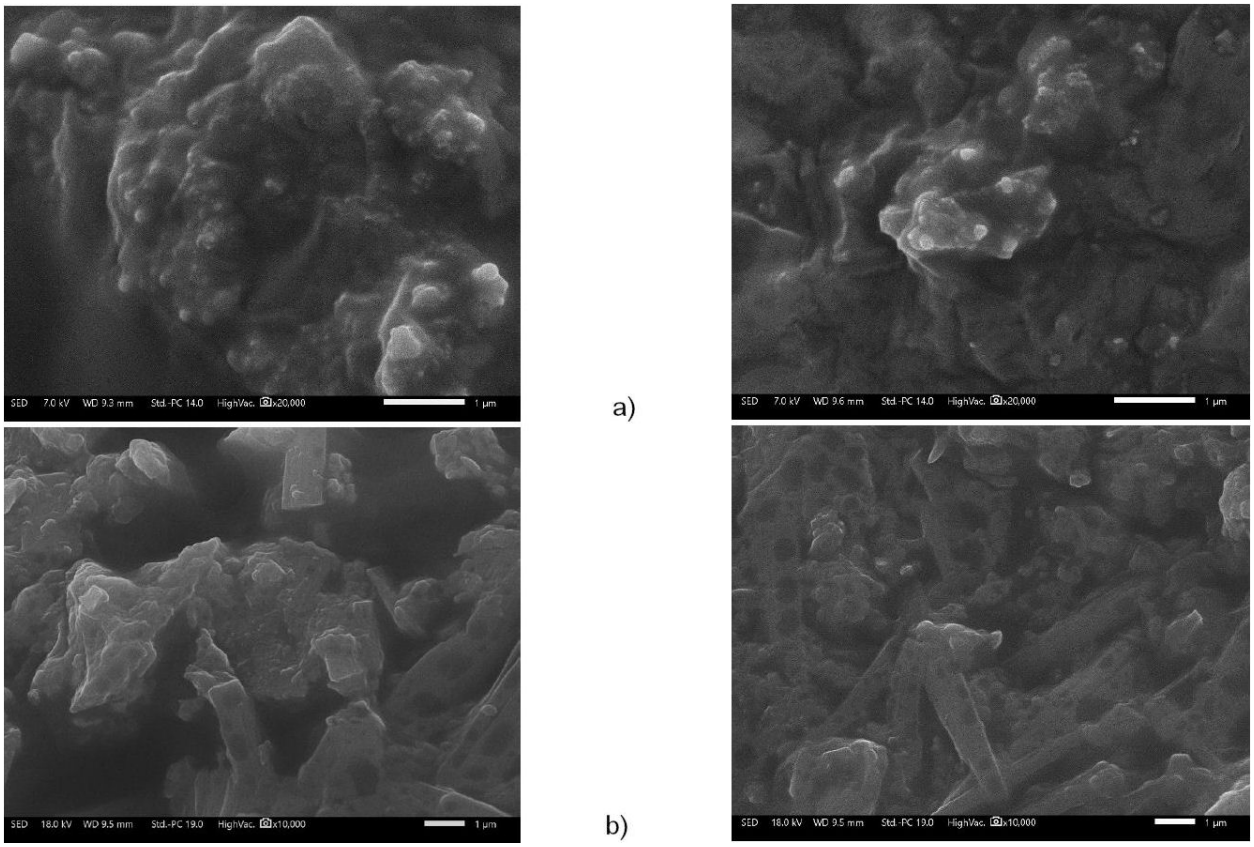

FIGURE 3. SEM images: a) GO without Fe_3O_4 assistance and b) GO with Fe_3O_4 assistance.

of Fe_3O_4 is necessary in the GO synthesis process using the LPE method.

LAS functions to reduce the interlayer tension of graphite, assisted by Fe_3O_4, which enhances the active surface area and provides magnetic separation capability for individual graphite layers [22,23,24]. LAS interacts with the oxygen-functionalized graphene surface, thereby physically reducing the surface energy of the solution and weakening the van der Waals forces between graphite layers, which consequently lowers the external force required to separate the graphite layers [22]. The cavitation effect generated by ultrasonication induces vibrations that mechanically separate the durian peel waste graphite layers previously weakened by LAS and Fe_3O_4 [25].

Ultrasonic cavitation originates from the formation of micro-vacuum bubbles within a liquid as a result of elastic pressure fluctuations induced by ultrasonic waves. Subsequently, these bubbles grow until they reach an unstable condition and then collapse implosively, generating high-pressure shock waves and microjets in their surrounding en-

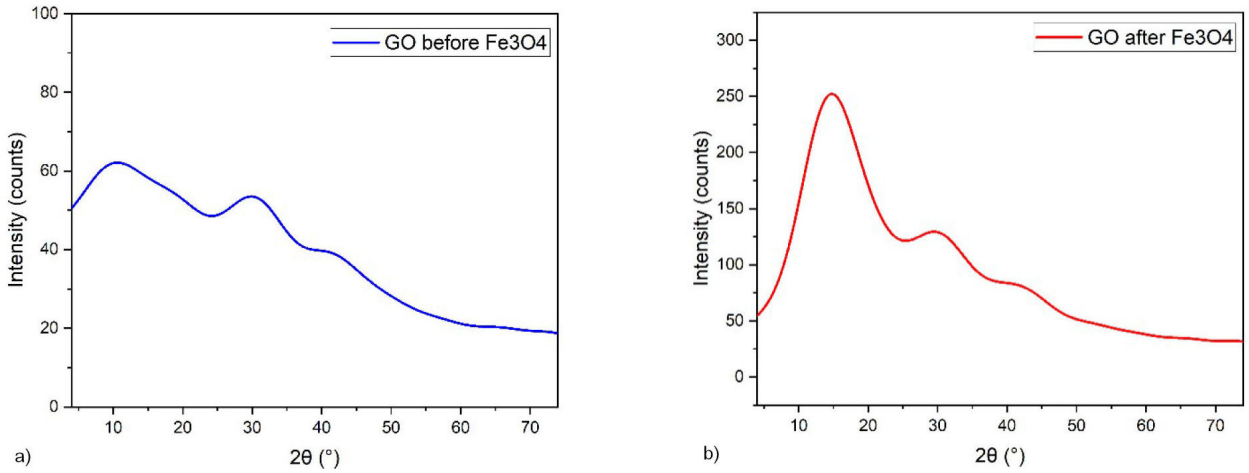

FIGURE 4. XRD diffractograms of GO: a) GO without Fe_3O_4 assistance and b) GO with Fe_3O_4 assistance.

vironment [26]. Importantly, the mechanical energy released during bubble collapse is substantially greater than the van der Waals forces, thereby overcoming the interlayer attractive forces of graphite and mechanically producing thin GO sheets [27].

Moreover, Fe_3O_4 is capable of reducing the surface tension of the solution by 42% compared to pure water. This enables Fe_3O_4 to modify the local pressure distribution during sonication, such that the collapse of ultrasonically induced bubbles generates shock waves that more effectively disrupt the interlayer interactions of graphite [28]. Therefore, the combined effect of surface tension reduction through the adsorption of LAS and Fe_3O_4 particles, together with the intense mechanical forces generated by ultrasonic cavitation, creates an energetic environment that is physically capable of disrupting the interlayer forces of graphite and facilitating the formation of graphene oxide. Figure 1 presents the GO sample synthesized with the assistance of Fe_3O_4.

Figure 2 shows the Raman spectra of the GO samples. GO synthesized without Fe_3O_4 assistance [Fig. 2a)] exhibits typical GO characteristics, as indicated by the presence of the D ($\sim$ 1350 cm^{-1}), G ($\sim$ 1580 cm^{-1}), and 2D ($\sim$ 2700 cm^{-1}) bands, with a relatively high I(D)/I(G) ratio suggesting a high degree of oxidation [29]. However, in GO synthesized with Fe_3O_4 assistance [Fig. 2b)], these bands are not clearly observed. This phenomenon may be attributed to dominant Raman signals being masked by sample fluorescence or a high background signal [30].

SEM images (Fig. 3) reveal the morphology of graphite that has begun to exfoliate into GO sheets. A clear morphological difference is observed between GO synthesized without Fe_3O_4 assistance [Fig. 3a)] and GO synthesized with Fe_3O_4 assistance [Fig. 3b)]. The GO without Fe_3O_4 assistance shows initial exfoliation into sheets, but the extent is very limited, whereas the GO synthesized with Fe_3O_4 assistance exhibits more distinct sheet-like structures with relatively symmetrical, irregular rectangular shapes and the presence of several holes on the sheets.

In general, GO morphology is characterized by thin, sheet-like structures that are folded and wrinkled with a non-uniform surface, where wrinkles, folds, and visibly opened interlayer spacing reflect the presence of oxygen-containing functional groups and structural defects formed during the graphite oxidation process, resulting in a large surface area and a non-homogeneous two-dimensional structure [31,32,33,34]. Therefore, it can be concluded that GO synthesized with Fe_3O_4 assistance produces better-exfoliated GO sheets and exhibits a higher degree of oxidation compared to GO synthesized without Fe_3O_4 assistance.

The diffractogram presented in Fig. 4 indicates the absence of the characteristic sharp peak at $2\theta = 26°$, which confirms that the graphite structure has been effectively exfoliated and oxidized to form GO [35]. However, a difference in peak sharpness is observed between the diffractograms in Figs. 4a) and 4b). GO synthesized with Fe_3O_4 exhibits a sharper diffraction peak compared to GO synthesized without Fe_3O_4. This suggests that GO with Fe_3O_4 possesses a more ordered crystalline structure than GO without Fe_3O_4 [36]. Such peak sharpening occurs when a material consists of relatively large coherent diffraction domains (crystallites) with good lattice ordering, whereas peak broadening or flattening is associated with very small crystallite sizes and/or the presence of lattice strain and structural disorder, which lead to variations in the Bragg angle and broadening of the diffraction profile [37].

4. Conclusion

This study demonstrates that graphene oxide can be synthesized from durian peel waste through a combination of pyrolysis and LPE method. GO was successfully synthesized from durian peel waste graphite using the LPE method through the synergistic effects of LAS surfactant, Fe_3O_4, and ultrasonic cavitation. Raman analysis confirmed the typical structural

features of GO, while the absence of distinct Raman bands in Fe_3O_4-assisted GO was attributed to fluorescence or high background interference. SEM observations revealed that Fe_3O_4 significantly enhanced the exfoliation process, producing more well-defined, sheet-like GO morphologies with characteristic wrinkles, folds, and defects associated with higher oxidation levels.

Furthermore, XRD results demonstrated the disappearance of the graphite peak at $2\theta = 26°$, indicating successful oxidation and exfoliation, with sharper diffraction peaks in Fe_3O_4-assisted GO suggesting improved crystalline ordering. Overall, the incorporation of Fe_3O_4 during LPE effectively promotes graphite exfoliation and oxidation, resulting in GO with superior structural characteristics compared to GO synthesized without Fe_3O_4. The dual outcome of waste valorization and material innovation makes this route highly promising for future applications in energy storage, catalysis, and environmental remediation.

Acknowledgment

This research was funded by the Ministry of Higher Education, Science, and Technology of the Republic of Indonesia (Kemdiktisaintek) under the 2025 Beginner Lecturer Research Grant (PDP) scheme, based on Decree Number 126/C3/DT.05.00/PL/2025 and Agreement/Contract Number 0498.04/LL5-INT/AL.04/2025.

1. A. Gutiérrez-Cruz *et al*., A review of top-down and bottomup synthesis methods for the production of graphene, graphene oxide and reduced graphene oxide, *Journal of Materials Science* **57** (2022) 14543, https://doi.org/10.1007/s10853-022-07514-z
2. A. Jiříčková *et al*., Synthesis and applications of graphene oxide, *Materials* **15** (2022) 920, https://doi.org/10.3390/ma15030920
3. X. Chen *et al*., Mechanism of Oxidization of Graphite to Graphene Oxide by the Hummers Method, *ACS Omega* **7** (2022) 23503, https://doi.org/10.1021/acsomega.2c01963
4. B. W. Pratama *et al*., Enhancing Supercapacitor Cell Capacitance through Liquid-Phase Exfoliation Synthesis of Graphene, *Journal of Multidisciplinary Applied Natural Science* **5** (2025) 408, https://doi.org/10.47352/jmans.2774-3047.254
5. V. S. I. Negara *et al*., Graphene-Based Electrode Materials via Liquid Phase Exfoliation from Chicken Feather Waste, *Jurnal Fisika Unand* **14** (2025) 305, https://doi.org/10.25077/jfu.14.3.305-311.2025
6. A. Sanei *et al*., Biomass Derived Reduced-Graphene-Oxide Supported α-Fe2O3/ZnO S-Scheme Heterostructure: Robust Photocatalytic Wastewater Remediation, *Journal of Environmental Management* **332** (2023) 117377, https://doi.org/10.1016/j.jenvman.2023.117377
7. M. T. uddeen Safian, U. S. Haron, and M. N. M. Ibrahim, A Review on Bio-Based Graphene Derived from Biomass Wastes, *Bio Resources* **15** (2020) 9756, https://doi.org/10.15376/biores.15.4.Safian
8. F. Chen *et al*., Facile Synthesis of Few-Layer Graphene from Biomass Waste and Its Application in Lithium Ion Batteries, *Journal of Electroanalytical Chemistry* **768** (2016) 18, https://doi.org/10.1016/j.jelechem.2016.02.035
9. X. Wu *et al*., Ultrasonic Liquid Exfoliation for Producing Graphene Materials from Rice Stem: Investigating Cellular Components and Functionalities, *Ultrasonics Sonochemistry* **103** (2024) 106782, https://doi.org/10.1016/j.ultsonch.2024.106782
10. E. K. Sitepu *et al*., Calcined Biowaste Durian Peel as a Heterogeneous Catalyst for Room-Temperature Biodiesel Production Using a Homogenizer Device, *ACS Omega* **9** (2024) 15232, https://doi.org/10.1021/acsomega.3c09642
11. Y. Pu *et al*., Performance of Bioenergy Production from Durian Shell Wastes Coupled with Dye Wastewater Treatment, *Water* **16** (2024) 2688, https://doi.org/10.3390/w16182688
12. A. Manmeen *et al*., Biochar and Pyrolysis Liquid Production from Durian Peel by Using Slow Pyrolysis Process: Regression Analysis, Characterization, and Economic Assessment, *Industrial Crops and Products* **203** (2023) 117162, https://doi.org/10.1016/j.indcrop.2023.117162
13. A. Hadi *et al*., Graphene Nanosheets Preparation Using Magnetic Nanoparticle Assisted Liquid Phase Exfoliation of Graphite: The Coupled Effect of Ultrasound and Wedging Nanoparticles, *Ultrasonics Sonochemistry* **44** (2018) 204, https://doi.org/10.1016/j.ultsonch.2018.02.028
14. Y. Kim and J. Kim, Fabrication of Fe3O4 Coated Boron Nitride Nanoplatelets by Liquid-Phase Exfoliation for Thermally Enhanced Epoxy Composites via Magnetic Alignment, *Composites Science and Technology* **188** (2020) 107961, https://doi.org/10.1016/j.compscitech.2019.107961
15. A. Krzyszczak, M. P. Dybowski, and B. Czech, Formation of Polycyclic Aromatic Hydrocarbons and Their Derivatives in Biochars: The Effect of Feedstock and Pyrolysis Conditions, *Journal of Analytical and Applied Pyrolysis* **160** (2021) 105339, https://doi.org/10.1016/j.jaap.2021.105339
16. H. He *et al*., A New Structural Model for Graphite Oxide, *Chemical Physics Letters* **287** (1998) 53, https://doi.org/10.1016/S0009-2614(98)00144-4
17. J. P. Rourke *et al*., The Real Graphene Oxide Revealed: Stripping the Oxidative Debris from the Graphene-Like Sheets, *Angewandte Chemie International Edition* **50** (2011) 3173, https://doi.org/10.1002/anie.201007520

18. H. Gao *et al.*, Effect of Preparation Conditions on Mechanical, Dielectric and Microwave Absorption Properties of SiC Fiber/Mullite Matrix Composite, *Ceramics International* **45** (2019) 11625, https://doi.org/10.1016/j.ceramint.2019.03.034

19. M. Acik *et al.*, The Role of Oxygen during Thermal Reduction of Graphene Oxide Studied by Infrared Absorption Spectroscopy, *The Journal of Physical Chemistry C* **115** (2011) 19761, https://doi.org/10.1021/jp2052618

20. X. Huang *et al.*, Graphene-Based Materials: Synthesis, Characterization, Properties, and Applications, *Small* **7** (2011) 1876, https://doi.org/10.1002/smll.201002009

21. Z. Sun *et al.*, Preparation and Formation Mechanism of Biomass-Based Graphite Carbon Catalyzed by Iron Nitrate under a Low-Temperature Condition, *Journal of Environmental Management* **318** (2022) 115555, https://doi.org/10.1016/j.jenvman.2022.115555

22. D. Susanto, S. Husna, and W. S. B. Dwandaru, Cavitation Effect towards Graphene Oxide Synthesis using Liquid Phase Exfoliation Method Assisted by Linear Alkylbenzene Sulfonate, *Jurnal Fisika dan Aplikasinya* **21** (2025) 29

23. A. Arabpour *et al.*, Graphene Oxide-Enhanced ZnO@Fe3O4 Nanocomposite: Synthesis, Characterization, and Catalytic Performance, *Results in Engineering* **28** (2025) 107442, https://doi.org/10.1016/j.rineng.2025.107442

24. M. P. da Silva *et al.*, Synthesis of Superparamagnetic Fe3O4-Graphene Oxide-Based Material for the Photodegradation of Clonazepam, *Scientific Reports* **14** (2024) 18916, https://doi.org/10.1038/s41598-024-67352-8

25. D. Qin *et al.*, Influences of Inter-Bubble Interactions on Ultrasonic Cavitation Dynamics and Subharmonic Emissions in Viscoelastic Media with Nonlinear Elasticity, *Ultrasonics Sonochemistry* **121** (2025) 107541, https://doi.org/10.1016/j.ultsonch.2025.107541

26. Y. Xu *et al.*, Liquid-Phase Exfoliation of Graphene: An Overview on Exfoliation Media, Techniques, and Challenges, *Nanomaterials* **8** (2018) 942, https://doi.org/10.3390/nano8110942

27. Y. Liu *et al.*, Liquid Phase Graphene Exfoliation with a Vibration-Based Acoustofluidic Effector, *Micromachines* **14** (2023) 1718, https://doi.org/10.3390/mi14091718

28. S. Gal *et al.*, Surface Tension of Graphene/Fe3O4 Water-Based Hybrid Nanofluids, *Journal of Molecular Liquids* **417** (2025) 126630, https://doi.org/10.1016/j.molliq.2024.126630

29. A. C. Sparavigna, Graphene, Graphene Oxide and Carbon Nanotubes in Raman Spectroscopy, *International Journal of Sciences* **13** (2024) 1, https://doi.org/10.18483/ijSci.2773

30. F. Korinth *et al.*, Assessment of Shifted Excitation Raman Difference Spectroscopy in Highly Fluorescent Biological Samples, *Analyst* **146** (2021) 6760, https://doi.org/10.1039/D1AN01376A

31. L. Seromo, N. Greesh, and J. P. Mofokeng, Synthesis, Morphology, and Structural Properties of Graphene Oxide (GO) and Its Composites with Transition Metal Phosphates for Application in Water Purification: A Review, *Carbon Trends* **21** (2025) 100566, https://doi.org/10.1016/j.cartre.2025.100566

32. C. Ceballos-Alvarez *et al.*, Influence of Graphene Oxide on Mechanical and Morphological Properties of Nafion Membranes, *Nanomaterials* **15** (2025) 68, https://doi.org/10.3390/nano15010068

33. W. Gul *et al.*, Synthesis of Graphene Oxide (GO) and Reduced Graphene Oxide (rGO) and Their Application as Nano-Fillers to Improve the Physical and Mechanical Properties of Medium Density Fiberboard, *Frontiers in Materials* **10** (2023) 1206918, https://doi.org/10.3389/fmats.2023.1206918

34. P. Viprya, D. Kumar, and S. Kowshik, Study of Different Properties of Graphene Oxide (GO) and Reduced Graphene Oxide (rGO), *Engineering Proceedings* **59** (2023) 84, https://doi.org/10.3390/engproc2023059084

35. L. Yi *et al.*, The Janus Structure of Graphene Oxide and Its Large-Size Conductive Film Strip Pattern, *Nanomaterials* **14** (2024) 980, https://doi.org/10.3390/nano14110980

36. A. R. Widyanto and M. Nomura, Effect of Seed Size on Pervaporation Performances Through FAU Zeolite Membrane, *Membranes* **15** (2025) 355, https://doi.org/10.3390/membranes15120355

37. J. Bastida and P. Pardo-Ibañez, Applications of X-Ray Powder Diffraction Microstructural Analysis in Applied Clay Mineralogy, *Minerals* **14** (2024) 584, https://doi.org/10.3390/min14060584